Improvement in Identification Accuracy of a Failure Diagnostic System for a Reusable Rocket Engine

Fumihisa Nagashima[1], Hatsuo Mori[2], Yasuhiro Ishikawa[3], Masaki Sato[4] and Tomoyuki Hashimoto[5]

[1,2,3]*IHI corporation, Tokyo, 190-1297, Japan*
nagashima8492@ihi-g.com

[4,5]*JAXA, Miyagi, 981-1525, Japan*
sato.masaki@jaxa.jp

ABSTRACT

As a technology for safe and efficient operation of reusable rockets, we are developing failure diagnosis technology for reusable rocket engines. In order to follow the changes in rocket engine operating conditions, a failure diagnostic method which monitors an error vector: the difference between the predicted and measured values of the sensors was developed. The method contains anomaly detection by Mahalanobis distance and failure identification by support vector machines (SVMs). In this report, the suitable monitoring sensors of SVMs for each failure mode were selected by using design of experiments. By using selected sensors, the F-score of SVMs were improved in all failure modes. From the results of the orthogonal table experiments, it was supposed that sensors which show the difference in failure modes are important to distinguish failure modes. In addition, a failure classifier combined with SVMs using the suitable sensors for each failure mode was developed and demonstrated. The performance of the combined failure classifier with the suitable sensors was mostly greater than that with all sensors. However, degradation of the classification performance was also obtained. It is necessary to consider how integrate the results of SVMs which are trained individually.

1. INTRODUCTION

Reusable space transportation systems have been developed to realize low cost and high frequent space transfer. For efficient operation of reusable rockets, it is effective to automate monitoring and inspections during and after a flight. One method is health monitoring, but because a rocket engine which is one of the main components in a rocket is a complex system, the automation of its health monitoring is a key issue. A rocket engine does not generate a constant thrust but control its thrust during a flight to reduce acceleration and to adjust flight altitude depending on a mission. Therefore, a mechanism of following a change of operation states is necessary for a health monitoring system of a rocket engine.

For that purpose, an anomaly detection method for variable operation states which predicts state quantities in a little future from known ones and monitors the difference between measured values and predicted values was developed by Maru, Mori, Ogai, Mizukoshi, Takeuchi, Yamamoto, Yagishita and Nonaka (2018). This method enables anomaly detection independent of operating states by using predicted state quantities under a normal operating condition as a basis. Nagashima, Hashizume, Mori, Ishikawa and Hashimoto (2022) detected and classified critical failure modes for a rocket engine with high accuracy by combing anomaly detection by Mahalanobis distance (MD value) and failure classification by support vector machines (SVMs). In that study, misclassification of SVMs was observed in some failure modes. It was considered that detecting a change of sensor values became difficult because some failure affects only a part of sensor values. To address this problem, improvement of accuracy of a failure classification has been aimed by selecting suitable monitoring sensors for each failure mode. Here, selecting suitable sensors by using design of experiments for failure classification by SVMs are reported.

2. FAILURE DIAGNOSTIC METHOD

2.1. Error Vector

Maru et al. (2018) defined the deference between predicted values and measured values as an “error vector”. The schematic image of the error vector is shown in Figure 1. Sensor values under a normal operating condition are predicted from the immediately preceding measured values and monitor the difference between these predicted values and the actual measured values. Here, a simulator for predicting sensor values is defined as a “parity simulator”,

and a vector whose elements are the difference between predictions and measurements of sensors at a certain time is defined as an "error vector". Since, the error vector shows how much the measured values deviate from the expected values under a normal condition, it can monitor the target system health regardless of operating conditions.

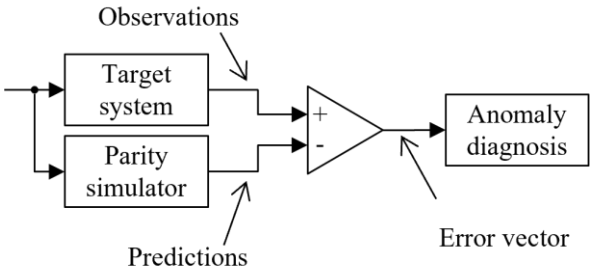

Figure 1. Concept of the error vector.

2.2. Failure Diagnostic System

Nagashima et al. (2022) proposed a combined method of anomaly detection by MD value and failure classification by SVMs for a failure diagnostic system of a reusable rocket engine. Anomaly detection by MD value can detect unknown anomalies because it determines whether the target system in normal. However, it cannot identify the location or the cause of the detected anomalies. Meanwhile, failure classification by SVMs can identify those of known failures, but it is difficult to detect unknown anomalies. Therefore, it is possible to detect unknown anomalies and identify known failure modes at the same time by first performing anomaly detection based on MD value and then classifying the detected anomalies using SVMs (Figure 2).

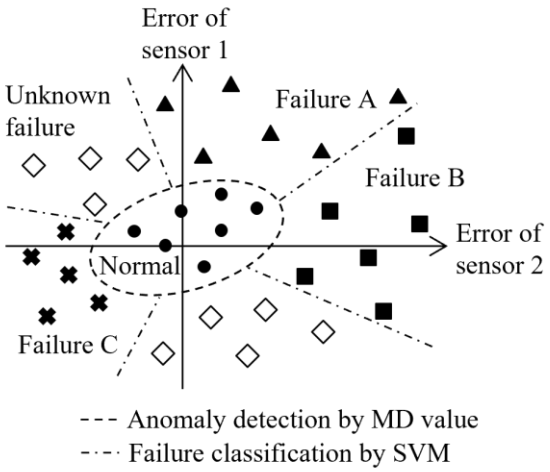

Figure 2. Failure diagnostic system by a combination of MD value and SVMs.

3. METHODOLOGY

3.1. Target Rocket Engine and Failure Modes

Machine learning requires a lot of training data, but in the case of rocket engines, the amount of operating data is often limited due to the enormous cost and time for implementation of rocket engine tests. In addition, it is not realistic to actually generate faults in order to acquire training data for failure classification. Therefore, a simulation-based development method (Nagashima et al, 2022) was used, which operating data used for machine learning are created using a simulator that reproduces a rocket engine. Figure 3 shows a system diagram of a target rocket engine. The simulator which creates training data was calibrated with operating data of rocket engine tests conducted at IHI Aerospace Aioi test facility (Ukai, Sakaki, Ishikawa, Sakaguchi and Ishihara, 2019).

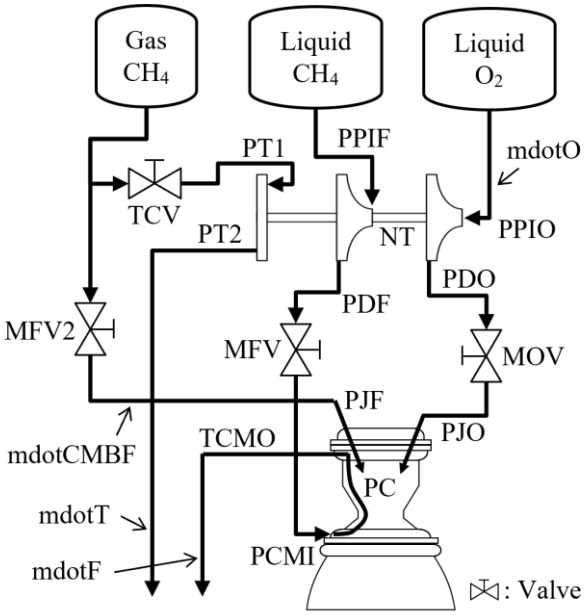

Figure 3. System diagram of the rocket engine.

In order to confirm the effect of improving the classification accuracy of SVMs by selecting the sensors, three failure modes are chosen as subjects of detection; a failure of the main oxidizer valve (MOV) and the main fuel valve (MFV), which misclassification occurred in the previous report (Nagashima et al., 2022), and a failure of the thrust control valve (TCV) that is also an electrically actuated valve. Failure modes included in the training data set and the test data set are listed in Table 1. The training data set has normal operating data (No. 0) as well as failure data not subject to detection (No. 4-6).

Table 1. Failure mode in data sets.

No.	Failure mode	Parameter	Magnitude
0	Normal	N/A	N/A
1	MOV insufficient opening	Opening rate	-30%
2	MFV insufficient opening	Opening rate	-30%
3	TCV insufficient opening	Opening rate	-10%
4	Damage on turbine blades	Efficiency	-10%
5	Cavitation in fuel pump	Pump head	-30%
6	Damage on injector elements	Pressure loss	-30%

3.2. Experiment

In order to select suitable sensors for each failure mode, an SVM that distinguishes one failure mode from a training data set was made for each targeting failure mode. That is, three SVMs with the suitable sensors for the failure of MOV, MFV and TCV were created.

Sensor selection for each failure mode was performed by assigning each sensor to an orthogonal table of an experimental design method. Each sensor was assigned as a control factor (Table 2), and two levels of "1: used" and "2: not used" were set. The experimental conditions were determined by allocating them to an L_{32} orthogonal table and a performance of an SVM in each experimental condition was investigated.

Table 2. Sensors used in failure classification by SVM.

Factor	Sensor	Explanation
A	PPIO	O_2 pump inlet pressure
B	PDO	O_2 pump outlet pressure
C	PJO	O_2 injector pressure
D	PPIF	CH_4 pump inlet pressure
E	PDF	CH_4 pump outlet pressure
F	PCMI	Coolant inlet manifold pressure
G	PT1	Turbine inlet pressure
H	PT2	Turbine outlet pressure
I	PJF	CH_4 injector pressure
J	PC	Combustion pressure
K	mdotO	Mass flow rate of liquid O_2
L	mdotF	Mass flow rate of liquid CH_4
M	mdotT	Mass flow rate of turbine gas
N	mdotCMBF	Mass flow rate of CH_4 injection
O	NTP	Rotation speed of turbopump
P	TCMO	Coolant outlet manifold temperature

The F-score, which is the harmonic mean of precision and recall, was used to evaluate the performance of the SVM. The precision is the proportion of data whose true values are positive out of the data predicted to be positive, and the recall is the proportion of data predicted to be positive out of the data whose true values are positive. By using the F-score, it is possible to consider both accuracy and sensitivity.

The hyperparameters of an SVM were optimized for each sensor combination. The tuning conditions of the hyperparameters are listed in Table 3. The SVMs were implemented by scikit-learn (Pedregosa, Varoquaux, Gramfort, Michel, Thirion, Grisel, Blondel, Prettenhofer, Weiss, Dubourg, Vanderplas, Passos, Cournapeau, Brucher, Perrot and Duchesnay, 2011) and the hyperparameter optimization was performed by Optuna (Akiba, Sano, Yanase, Ohta and Koyama, 2019).

Table 3. SVM hyperparameter tuning conditions.

Item	Condition
SVM module	Scikit-learn
Optimization framework	Optuna
SVM kernel	RBF kernel
Range of cost parameter	$10^{-5} < C < 10^{5}$
Range of kernel width	$10^{-5} < \gamma < 10^{5}$
Cross validation	5-fold cross validation
Scoring	F-score

4. Results and Discussion

4.1. Optimization of Sensor Combination

Figure 4 shows a factorial effect diagram of the F-score made from the orthogonal table experiment for each failure mode. In failure mode 1 (MOV insufficient opening), there is a large difference in the F-score depending on whether K: mdotO (oxidizer flow rate) is used. This indicates the importance of monitoring the oxidizer flow rate, which is directly affected by insufficient opening of MOV, and it can be said that a reasonable result was obtained. The sensor that has the next largest impact on the F-score is F: PCMI (regeneratively cooled chamber inlet pressure), but this measurement position is in a different line from MOV (Figure 3). Thus, PCMI is considered to be almost unchanged in failure mode 1. The reason why the unchanged sensor had a large impact on the classification score is that it is an effective sensor for distinguishing from other failure modes. Figures 5 and 6

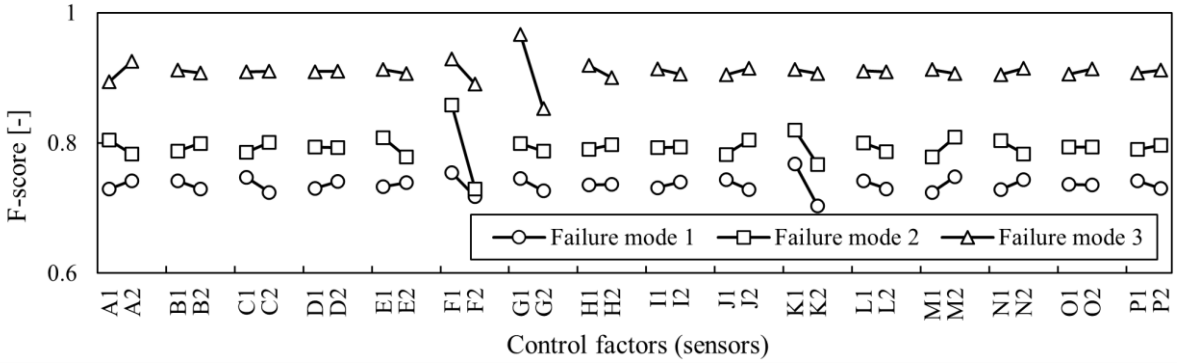

Figure 4. Factorial effect diagram of F-score, failure mode 1: MOV insufficient opening of -30%, failure mode 2: MFV insufficient opening of -30%, failure mode 3: TCV insufficient opening of -10%.

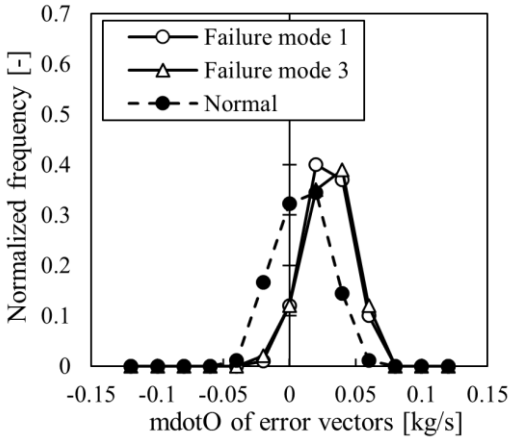

Figure 5. Frequency polygons of mdotO in the training data set, failure mode 1: MOV insufficient opening of -30%, failure mode 3: TCV insufficient opening of -10%.

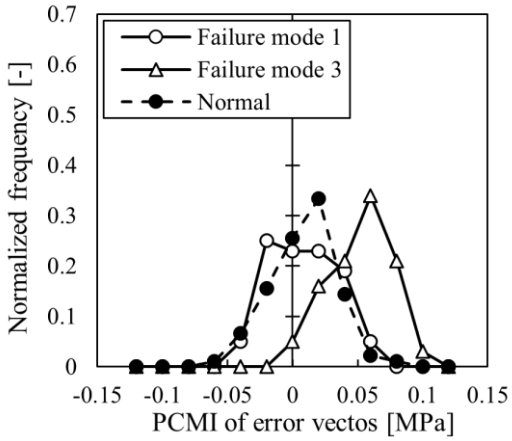

Figure 6. Frequency polygons of PCMI in the training data set, failure mode 1: MOV insufficient opening of -30%, failure mode 3: TCV insufficient opening of -10%.

show the distribution of mdotO and PCMI in the training data sets of normal and failure modes 1 and 3, respectively. Changes in the distribution of mdotO due to failures are similar in failure modes 1 and 3 as shown in Figure 5, making it difficult to distinguish between them. On the other hand, PCMI shows clearly different distributions in failure modes 1 and 3 as shown in Figure 6. In this way, it can be said that the sensor whose behavior differs between the target failure mode and the other failure modes also appears in the factorial effect diagram as an important sensor.

In failure mode 2, the effect of F: PCMI is the largest, and this is because the effect of insufficient opening of MFV appears as a change in pressure on the downstream side. K: mdotO has the second largest effect, but it is supposed that this is not because of the MFV failure, but because it is effective in distinguishing it from other failure modes. Failure mode 3 affects more sensors than failure modes 1 and 2 because the pump side is also affected by the reduced turbine output. It is considered that G: PT1 and F: PCMI, which have large changes due to the failure, greatly contributed to the classification performance.

For failure modes 1 and 2, it was found that not only sensors that directly indicate the effect of the failure, but also sensors that show the difference from other failure modes are necessary for failure classification. Sometimes only the sensors which are directly affected by a failure are used for failure detection, however this result indicates that sensors which show the difference in failure modes are also important.

All the sensors that the F-score was increased by using them were selected from the factorial effect diagram as suitable sensors for failure identification of each failure mode. Figure 7 shows the F-scores when using all sixteen sensors and when using only the suitable sensors for each failure mode. Using the suitable sensors resulted in better classification performance in any failure mode. It is assumed that the characteristics of each failure mode have become easier to grasp by reducing the number of monitoring sensors.

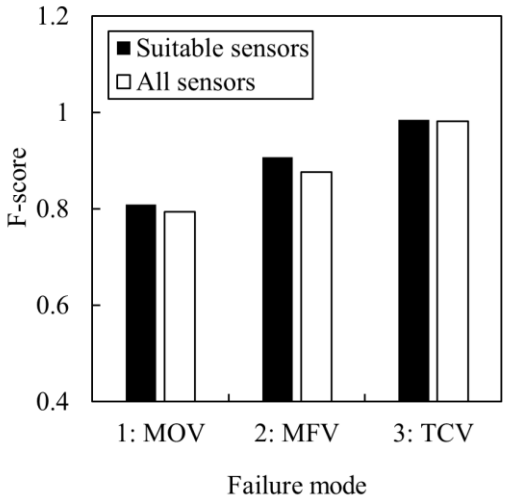

Figure 7. F-scores by the optimal sensor combination, failure mode 1: MOV insufficient opening of -30%, failure mode 2: MFV insufficient opening of -30%, failure mode 3: TCV insufficient opening of -10%.

4.2. Combined Failure Classifier

By combining the SVMs with the suitable sensors for each failure mode, a failure classifier that identifies the three failure modes (1, 2 and 3 in Table1) is created. As the classification result of the combined failure classifier, the one with the largest decision function calculated by each SVM was adopted. Figure 8 shows the classification scores of the failure classifier created using all sensors and the suitable sensors. In failure mode 1 and 3, the F-score was improved by using only suitable sensors, but in failure mode 2, the classification performance was better when all sensors were used. Since the performance of the single SVM for the failure mode 2 is higher than when all sensors are used, it is supposed that the degradation of classification performance is caused by misclassification of other SVMs. In other words, the SVM of the failure mode 2 classified correctly but other SVM misclassified with larger decision function, so the combined failure classifier adopted a wrong classification result. The hyperparameters were optimized individually for each SVM because the sensor combinations and the data distribution are different in failure modes. Considering how integrate classification results with taking account of the difference of SVMs for each failure mode is a future issue.

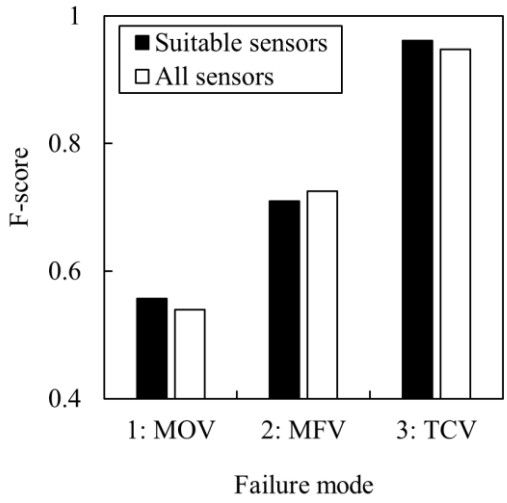

Figure 8. F-scores of combined failure classifier, failure mode 1: MOV insufficient opening of -30%, failure mode 2: MFV insufficient opening of -30%, failure mode 3: TCV insufficient opening of -10%.

5. CONCLUSION

The suitable monitoring sensors of failure classification by SVMs were selected for each failure mode by using design of experiments. The failure classification performance of SVMs was improved by selecting suitable sensors for each failure modes. The effect of a failure becomes clearer by reducing sensors. In addition, it is supposed that sensors which show the difference in failure modes are important to identify failure modes.

However, the degradation of the performance of failure classifiers was obtained for failure mode 2 when the classification results of SVMs tuned with different sensor combinations for each failure mode were integrated. Therefore, in the future, it is necessary to consider how integrate the classification results of SVMs with the suitable sensors selected for each failure modes.

REFERENCES

Akiba, T., Sano, S., Yanase, T., Ohta, T. & Koyama, M. (2019). Optuna: A next-generation hyperparameter optimization framework. Proceedings of the 25th ACM SIGKDD International Conference on Knowledge Discovery & Data Mining (pp.2623-2631), August 4-8, Anchorage AK, USA. doi: 10.1145/3292500.3330701

Maru, Y., Mori, H., Ogai, T., Mizukoshi, N., Takeuchi, S., Yamamoto, T., Yagishita, T., & Nonaka, S. (2018). Anomaly detection configured as a combination of state observer and Mahalanobis-Taguchi method for a rocket engine. *Transactions of the Japan Society for Aeronautical and Space Sciences, Aerospace Technology Japan*, vol. 16 (2), pp. 195-201. doi: 10.2322/tastj.16.195

Nagashima, F., Hashizume, T., Mori, H., Ishikawa, Y., & Hashimoto, T., (2022). Development of failure diagnostic system for a reusable rocket engine using simulation. *SICE Annual Conference 2022* (ThB07.3), September 6-9, Kumamoto, Japan.

Pedregosa, F., Varoquaux, G., Gramfort, A., Michel, V., Thirion, B., Grisel, O., Blondel, M., Prettenhofer, P.,

Weiss, R., Dubourg, V., Vanderplas, J., Passos, A., Cournapeau, D., Brucher, M., Perrot, M., & Duchesnay, E. (2011). Scikit-learn: Machine learning in Python. *Journal of Machine Learning Research*, vol. 12, pp. 2825-2830.

Ukai, S., Sakaki, S., Ishikawa, Y., Sakaguchi, H., & Ishihara, S. (2019). Component tests of a LOX/methane full-expander cycle rocket engine: Injector and regeneratively cooled combustion chamber. *8th European Conference for Aeronautics and Space Sciences*. July 1-4, Madrid, Spain

Fumihisa Nagashima is an engineer in IHI Corporation. He received a Ph. D in Mechanical Engineering from Tokyo Institute of Technology, Tokyo, Japan, in 2021. His work focuses specifically on real-time health monitoring of reusable rocket engine.